(2)

ONR Grant No. N00014-90-J-4077

Relaxor Ferroelectrics for Electrostrictive Transducer

Quarterly Report

(Period) September 1991-January 31, 1992

Sponsored by

Office of Naval Research (ONR)

Submitted to:

Dr. Robert Ting
Navy Research Laboratory
Underwater Sound Ref. Division
Box 8337
Orlando, FL 32856

Submitted by:

Thomas R. Shrout

Sei-Joo Jang

Materials Research Laboratory
Penn State University
University Park, PA 16802

Distributed to:

Mr. Norman Meeks

Dr. Wallace Smith

INTRODUCTION

Objectives

The objective of this program is to investigate the potential of electrostrictive actuator materials for use in NAVY-type sonar. The anticipated performance requirements for such materials is summarized in the following:

- Operating temperature range 0-30°C
- High sensitivity; i.e. large E-field induced strain (>0.03%)
- Minimal hysteresis (<10%) and low loss (<1-2%)
- Frequency of operation ≤ kHz
- Mechanically stiff (low compliance)

Additional requirements include (1) operational E-field (~10 KV/cm), (2) strain under prestress, and (3) duty cycles; ~10% (5 seconds drive them off for 1 minute).

As stated above, the electromechanical coupling proposed is "electrostriction," in contrast to the currently used piezoelectric phenomena. Analogous to the Navy Type I, II, etc., piezoelectric classes, the electrostrictive materials investigated have been categorized and presented in Table I.

Recent studies on electrostrictive materials have changed the evaluation of their usefulness, for the following reasons in particular: reduced hysteresis of polarization and strain, reduction of ageing effects and "walk off," large field-induced strains, and good reproducibility under cyclical electric field drive. Electrostrictors can become piezo-active with a biasing field to induce large effective piezoelectric coefficients and more linearized strain field response.

The basis for selection of the material families becomes obvious upon examining the expression for the E-field induced piezoelectric phenomena given as:

$$d_{ind} = 2Q \varepsilon_o K_3 P_{ind} \qquad (1)$$

where Q is the electrostrictive polarization coefficient, ε_o the permittivity of free space (8.85 x 10^{-12}) F/m, K_3 the dielectric permittivity and P_{ind}, the E-field induced polarization. Naturally, to obtain a large induced piezo d coefficient requires (1) a large electrostriction coeff. Q, (2) large K,

and (3) large induced polarization. Relative values of each are summarized in Table II for four classes of materials selected in this program.

Efforts have been made to ascertain the delineating borders between the Regimes of Electromechanical Behavior :

- **Region I. Piezoelectric (T < Td)**

- **Region II. Micro-Macrodomain (Td < T < Tm)**

- **Region III. Electrostrictive (T > Tm)**

Region I materials have a stable remanent polarization (P) and large associated strain levels which have "butterfly" strain-E field loops. The increase of remanent polarization/strain however, leads to increased hysteresis and "walk off" reducing the difference between the maximum induced strain and the initial position due to the remanent strain offset.

Region II materials are those relaxor materials which are located in a regime where nanometer-scale domains greatly influence the behavior of polarization/electromechanical properties. The polarization fluctuations arising from thermal motions around and just below the broad *ferroelectric phase transition are a critical parameter.* Their size is linked with chemical inhomogeneity, cation ordering, and the electric dipolar field interactions between themselves and the polarizable crystal lattice. In this regime, the micro polar regions couple strongly with each other but not the nonpolar lattice, thus their polarizability is effectively large under electric field, leading to large electric permitivities and large electrostrictive strains from micro/macrodomain reorientation.

Region III electrostrictive materials are those which operate above the dielectric constant maximum temperature and are characterized by non-hysteretic strain and polarization field loops. The strain electric field response is primarily nonlinear and quadratic. The absence of macroscale domains implies reduced ageing, lack of remanent strain, improved reproducibility, and slim-loop ferroelectric response. The level of field-induced strain is somewhat reduced as compared with Region II micro/macrodomain operation, but the trade-off of reduced hysteresis if adequate displacement can be achieved for a given field level is the basis for useful transducers of this type.

Though electrostrictive Q values are low for relaxor ferroelectrics, their intrinsically large K_3 and relative low E-field dependence provides for large induced polarizations, becoming greater in the micro-macro polar thermal region designated $\underline{T_m\text{-}T_d}$ region. It is again this region that results in the large strains in the Type II relaxors, or PLZT family which thermally functions in the micro-macro regime. Though the electrostrictive coefficients are the largest for the normal Type III

and IV families, along with large K_3, the level of P_{ind} is reduced owing to a large E-field dependence of the dielectric constant. In terms of working temperature range, i.e. large strain, minimal temperature dependency, and low hysteresis. The large Curie-Weiss constant of the relaxor Type I reflects a broad and diffuse transition, along with a relative large (T_m-T_d) differences, and is even more broadened in the PLZT type family. As expected, with T_m equal to T_d for normal ferroelectrics limits their temperature usage being further narrowed by their sharp dielectric maxima as given by the Curie-Weiss values.

Table I
Classification of Electrostrictive-Based Transducers

Classification	Family
Type I	$Pb(B_1B_2)O_3$ - Relaxor ferroelectric e.g. $Pb(Mg_{1/3}Nb_{2/3})O_3$ Relaxor - Quasiferroelectrics
Type II	$Pb_{1-y}La_y(Zr_{(x)}Ti_{(1-x)})O_3$-PLZTs $y \geq 0.7$ $x \geq 0.65$
Type III	$Ba(Ti_{1-x}Sn_{(x)})O_3$ $x \geq 0.1$ Pinched Ferroelectrics (Normal)
Type IV	$Ba_{1-x}Sr_{(x)}TiO_3$ Normal Ferroelectric Note: (x) depends on operational temperature e.g. R.T. paraelectric $x > 0.3$

It is the purpose of this report to update the progress of the investigation with emphasis on the groups (types) of electrostrictors with special relevance to the requirements of NAVY sonar transducers.

EXPERIMENTAL PROCEDURE

Details of the fabrication of the various sintered ceramics were described in the previous reports. Specific modifications to the processing of the various materials included the following:

Table II

Relevant Electro-Mechanical Parameters for E-field Induced Piezoelectrics

Classification	Piezo-Strains (x) (longitudinal)	Q_{11}-Q_{12} m^4/C^2	K_{max} x 10^3	T_{max}/T_d	Curie Const $C(x10^5)$*	$P_{10\ md}$ (E = 10kV/cm) (C/m^2)	Physical Properties E. Comp./Therm.Exp. s^E_{ii} ($x10^{-12}\ m^2/N$)	α $x10^{-6}/°C$
Type I PMN- Based	0.1%	0.01	20 - 30	$T_m > T_d$	~ 5	.15-.20	8-10	1-2
Type II PLZT	0.1%	.01-.012	6-8	$T_m >> T_d$	~6-9	.15-.25	9-13	~5
Type III $Ba(Ti,Sn)O_3$	0.07%	.10-.20	~30	$T_m = T_d$	2-4	.08-.15	4-6	10
Type IV $(Ba,Sr)TiO_3$	0.05%	~0.1	~15	$T_m = T_d$	1	.---	4-6	10

*Ref. Uchino et al, 1980

Type I	Relaxors	Annealing @900°C-Air	(1) Minimize aging (2) Maximize K
Type II	PLZTs	Hot-Pressed and Conventionally Sintered (Annealed)	
Type III	$Ba(Ti_{1-x}Sn_x)O_3$	Pre-reacted B-sites, Quenching (compositional ordering)	
Type IV	Ba_{1-x}, Sr_xTiO_3	High Purity Raw Materials and High Energy Mixing/Milling (compositional homogeneity)	

Further processing optimization is ongoing to minimize microstructural defects, e.g. grain size, porosity, and grain boundary phases. Post annealing at 900°C for 6 Hrs.in air for the sintered ceramic samples was also undertaken after sintering to facilitate uniformity of processing kinetics and maximize dielectric constant behavior.

Compositional modifications made for the various types of electrostrictors includes the following:

Influence		Modification	Reason / Property
Type I	$Pb(Mg_{1/3}Nb_{2/3})O_3$ [PMN] (w / Cation Modifications)	• Ti^{+4}	• Shift T_{max} upward
		• Sr^{+}, Ba^{+2}, Ca^{+2}	• Shift T_{max} downward • Effect $\Delta T = T_{max} - T_d$
		• La^{+3}	• $\uparrow \Delta T = T_{max} - T_d$ • Inhibit grain growth • Shift T_m downward
Type II	$Pb_{1-y}La_y(Zr_{1-x}Ti_x)O_3$	• Increase La$\uparrow$ y	• Shift T_m downward • $\uparrow \Delta T_{m-d}$
		• Vary x	• Shift T_m
Type III	$Ba(Ti_{1-x}Sn_x)O_3$ x=0.13	• None	
Type IV	$Ba_{1-x}Sr_x(Ti)O_3$	• Vary x	• Shift T_m

Electrical Characterization

Electrical characterization of the materials fabricated to date include the following:

- K vs. temperature and frequency (100 Hz, 1 kHz, 10 kHz, and 100 kHz.
- Dielectric Loss (same as above)
- T.C.C. (Temperature Coefficient of Capacitance)
- Strain vs. E-field @ 0.1-100 Hz and temperature (resistive strain gauge technique) and selected Interferometer measurements (1Khz)
- Polarization (P) vs. E-field (as above) in conjunction with the str.. :-field loops

In view of the stated purpose for the application frequency requirement (≤ 1 kHz), higher frequency measurements of the strain (x) and polarization (P) were made on selected samples of Type I and II relaxors. It is important to note that frequencies higher than 1 Hz for the strain gauge technique require optimum bonding of the resistive gauge and extreme care must be taken to insure an elastically responsive deformation. As such, only frequencies up to 100 Hz have been made.using this technique along with a Sawer-Tower circuit for dielectric polarization measurements. Higher frequencies (100 - 1 kHz), require a Kyowa 300 model Wheatstone Bridge, which is under repair or alternatively the Mach-Zender strain interferometer as reported here for the PLZT (9/65/35) composition (1Hz - 1kHz).

Higher frequency measurements (100 kHz to 5 MHz) were performed using standard Resonance-Antiresonance techniques, whereby a blocking capacitor is incorporated to allow high D.C. bias voltages. From these measurements, one can obtain the induced piezo-coupling coefficients (k_t and k_p) mechanical Q, and elastic compliance s_{11}^E as a function of field. The elastic compliance data was then used to investigate the strain under prestressed loading conditions for the relaxor compositions basd upon their measured strain levels with a given field (typically 10kV/cm).

Along with the above, an additional requirement of the proposed electrostrictors is their performance under an applied load or stress. In order to evaluate the electromechanical behavior of the materials under significant load stress, field-induced strains were measured under known stress levels from applied weight loads by the linear voltage differential transform (LVDT) method. The deflection of a metal rod with an insulating end tip of known area could be used to find the characteristic stress-strain curves for these relaxor ceramic compositions. The longitudinal strain measurements also were eva;luated by an elastic constant measurement for given initial (deformation) strain and field level. The Poisson ratio (- s_{11}/s_{12}), relating the longitudinal and transverse compliances, indicates along with the higher induced strain levels for the longitudinal configuration that it is the appropriate geometry for stress-strain load line behavior for Navy sonar

applications under prestress. To estimate the load carrying ability of the various types of relaxors, the elastic compliance (s_{11}^E) determined from the resonance techniques in conjunction with strain measurements was used to calculate anticipated loadline performances. In every case there is a trade-off betwen desired levels of strain induced and the maximum pressure (stress) which can be pushed against for a given electric field.

The ferroelectric spontaneous polarization (P) was measured by the Byer and Roundy method. Thin ceramic polished disc specimens were electroded and cooled under E-field poling from above the temperature of dielectric constant maximum to below -150°C. After removing the DC field and neutralizing the surface space charges, the poled samples were heated at a constant rate of 2 degrees per minute while recording the pyroelectric current. The pyroelectric coefficient (p_i) = ($P_i = p_i\, dT$) was calculated from the pyroelectric current:

$$p = \frac{i}{A(dT/dt)} \left[\frac{c}{m^2\, {}^0K}\right] \qquad (2)$$

where i is the pyroelectric current, A the electroded area, and dT/dt the heating rate. The polarization was then calculated by integrating the pyroelectric coefficient

$$P_s = \int p\, dT \quad \left[\frac{c}{m^2}\right]. \qquad (3)$$

Dielectric constant measurements were carried out as described previously using an LCR meter to obtain the capacitance, dielectric constant, and dielectric tan δ losses.

Results and Discussion

The results presented are divided into the different types of electrostrictors. Since most of the work to date has been on Type I & II relaxors, they will be presented first. With the presentation of data, the theme of "commonality" within the classes is emphasized as well as engineered intrinsic changes made through compositional modifications. At the end of the section, the different types of electrostrictors will be contrasted.

Type I Relaxor Ferroelectrics - $Pb(B_1B_2)O_3$

The dielectric and polarization behavior for several relaxor ferroelectrics based on PMN-PT engineered in this work are presented and summarized in Figures 1-4 and Table 3. The common

area inhabited on the Figure 1 diagram shows that with adequate processing the consistent trend for the dielectric constant maximum will, as presented, track with the temperature T_m at which this maximum occurs within a given compositional family. The $PbTiO_3$ modifications (Figure 2) shift T_m linearly upwards (~5°C/mole%) whereas Ba^{+2},Sr^{+2},La^{+2} shift T_m downward (~25°C/mole%). The range of Region II behavior decreases as the morphotropic phase boundary is approached in PMN-PT (Figures 3 and 4). Naturally, a combination of both $PbTiO_3$, or Ti^{+4}, on the perovskite B-site and one of the A-site modifiers can also be employed. An example of this is for the relaxor $Pb(Mg_{1/3}Ta_{2/3})O_3$ upon which the Nb cation is replaced by Ta^{+5}, which lowers T_m to about -100°C, but with the addition of 27 mole% $PbTiO_3$ can be shifted to near room temperature without significantly changing the dielectric constant maximum. Dielectric commonalities of the role of modifiers on the dielectric constant maximum K_{max} and the temperature at which it occurs T_{max}, are summarized in Tables IIIa,b,c for the various cation dopants of PMN-PT.

The lanthanum addition to the PMN-PT ceramics has been shown to both widen and lower the temperature range of Region II micro/macro domain (T_m-T_d) behavior in near MPB compositions (Kim, 1990). The same trend is seen in Figure 5 for the lower $PbTiO_3$ amounts (0% - 7%) of this study. This is evidently the causation of the relatively large region of large but nearly nonhysteretic field induced strain observed in this temperature regime.

Increasing $PbTiO_3$ amounts in PMN-PT ceramics not only raises the dielectric constant maximum temperature but the depolarization temperature T_d also and more effectively so that the Region II behavior occurs in a narrower range and at higher temperatures. Ba and Ca addition also decreases the difference between the T_m and T_d temperatures (Figures 1,6).

Additional modifications were made for relaxors Type I, specifically the replacement of PMN with $Pb(Ni_{1/3}Nb_{2/3})O_3$ (PNN), $PbTiO_3$ (PT), and $Pb(Zr_{0.53},Ti_{0.47})O_3$ (PZT) in order to investigate the PNN-PZT system. The $Pb(Ni_{1/3},Nb_{2/3})O_3$-$Pb(Zr_{0.53},Ti_{0.47})O_3$ compositions were examined and found to show increasing polarization for increasing amounts of PZT added shifting T_d to higher temperatures.

Type II $Pb_{1-x}La_x(Zr_{1-y}Ti_y)O_3$

The PLZT relaxors of the (X/65/35) series with X= 9,10,11 have been investigated for their dielectric, polarization, and electromechanical response (Meng et al, 1985; also see previous reports). Based upon the measured properties as summarized in Table 4, the PLZT type electrostrictors have features which distinguish them from the other types examined previously.

The dielectric constant peaks (6000 - 9000) (although not as high as the Type I) are quite broad and maintain a high value over a large range. (Fig.5.). Dielectric losses (tan δ ~.05 -.06) are also lower than that observed in the PMN-PT Type I dielectrics. Lanthanum addition lowers the temperature of T_m and the K_{max}. values. for this series as well. The field induced saturation and eventual lowering of the dielectric constant (Pan et al, 1989) is not as appreciable as in other perovskite electrostrictors and the dielectric constant in fact increases with field to a certain extent in the relaxor (Region II) regime.

Polarization as a function of temperature is shown in Fig.7 for the chosen PLZT compositions as measured by the Byer - Roundy technique. The PLZT (9/65/35) composition has the highest polarization values of those investigated. The T_d value decreases with La^{3+} and even more rapidly than does T_m for a given composition. This leads to an increased range for PLZT region II behavior among the electrostrictor types examined (T_m-T_d > 125°C).

Measuring the longitudinal strain by the Mach - Zender interferometer strain ultradilatometer for the PLZT (9/65/35) composition leads to the longitudinal strain vs. frequency curve shown in Figure 8. The dispersion of the strain response is of the order observed previously (Zhang et al, 1989) and is somewhat more dispersive than that of the PMN-PT compositions.

Stress-Strain Behavior of Relaxor Ferroelectrics

The measured displacement of a ceramic actuator or sonar under loaded (prestressed) conditions can establish the relationship between elastic electrostrictive and compliance behavior. Relaxor ferroelectric transducers can generate large strains and large forces but a trade-off between the two is in effect for any given driving field. The linear relationship at modest loads between the stress and strain (Hook's Law) implies a generalized elastic constant coefficient

$$(\text{Strain}) = (\text{Electrostrict. Coefficient})(\text{Polarization})^2 + (\text{Elast. Compliance})(\text{Stress}).$$

or specifically in reduced tensor form for perovskite material symmetry,

$$X_1 = Q_{12} P^2_2 + S_{12} X_2 \qquad \text{(longitudinal strain)} \qquad (4)$$

$$X_2 = Q_{11} P_1 + S_{22} X_2 \qquad \text{(transverse strain)} \qquad (5)$$

where the prestressing transverse or longitudinal loads are represented by the X and the S_{ij} are the elastic compliances. Strain hysteresis loops were undertaken while the electrostrictively induced strains of the sample pushed against the load,.thus the measurement only accounts for that component of the total field and load induced deflection. The electromechanical coupling and elastic constants by resonance measurements method from obtained values of the Young's modulus and Poisson ratio can be used as a check on the measured elastic compliances of the strain/force loadline slopes by the direct LVDT method.

The stress-strain response (Figure 9) under applied load for PLZT (9/65/35) in the longitudinal strain configuration were calculated by the measured longitudinal strains by LVDT method at lower stress loading and the elastic compliances (s^E_{11}) from the resonance measurements of thin electroded samples. The calculated load line curves indicate that the PLZT compositions have initial high strain levels and can push a considerable load (>20MPa) and still maintain a reasonable strain level. The effective compliance from the resonance measurements of $s^E_{11} = 9.95 \times 10^{-12}$ m^2/N were employed in the calculations of the loadlines .

The Type I PMN composition (figure 9b) has a higher stiffness (response under field and load) than does the elastic response of the PLZT (9/65/35). The PMN elastic constants at an electric field of about 10 KV/cm by the resonance technique were $s^E_{11} = 8.4 \times 10^{-11}$ m^2/N. The ceramic Poisson Ratio (σ^E) of 0.299 was measured for this field level..

Type III $Ba(Ti_{1-x}Sn_x)O_3$ x=0.13

The solid solution system Ba(Ti,Sn)O3 (BTS) was one of the earliest ferroelectrics examined with a diffused phase transition (Smolenskii, 1954). Initial investigations on the electromechanical properties of BTS have shown several interesting features (Cieminski and Beige, 1991). The $Ba(Ti_{.87}Sn_{.13})O_3$ composition was chosen for examination because of its relatively large strain levels and the lack of significant hysteresis in the desired temperature range.

The dielectric constant of BTS (0.87 / 0.13) had a value exceeding 30,000 at 1 kHz and a transition temperature of 7.6° C, as can be seen in Figure 10. The dielectric constant peak is diffused by the addition of Sn (FWHM of 22° C) and is not greatly dispersive with regard to the increase of T_m with frequency. The dielectric constant examination for this composition is larger than that reported by Ciemenski (1990). Polarization as a function of temperature for BTS for the given preparation parameters are indicated in Figure 11.

The polarization and transverse strain as a function of electric field hysteresis loops for this BTS composition is shown in Figure 12 a-e for various temperatures where the strains were measured using the strain gauge technique and a Sawyer-Tower circuit for the ferroelectric polarization. Table 5 gives averaged strain levels S_{10} and S_{20} along with the amount of hysteresis observed for the measured temperatures.

$Ba(Ti_{.87}Sn_{.13})O_3$ dielectric hysteresis loops differ from the relaxor types in having extremely nonlinear P-E behavior with substantial dP/dE near the coercive field and large effective low E-field dielectric constant which, because of the saturation at high field implies variation of the dielectric permittivity with E-field dependence.

The amount of strain hysteresis decreases with increasing temperature and is in accord with the temperature coefficient of capacitance and the domain formation in this material as indicated in the previous figure.

The field induced strain, although not as large as in the Group I and Group II. is at lower field levels capable of producing a nearly linear (almost piezoactive) response without significant remanent strain offset. The effective field electrostrictive coefficients are thus larger in comparison to the other groups.

Compared to Pb based relaxors, however, the levels of polarization (both spontaneous and field induced) are lower, Fig.11-12, and consequently, the effective induced strain levels, according to the phenomenology, are lowered as well. The values of induced strain S_{10} for large fields (> 10 kV/cm) are not as large as the Pb based family of relaxors (Fig.12 and Table 5) but other features make this composition and solid solution system notable for electromechanical / strain transducers:

1) A nearly linear strain-E field behavior at modest field followed by a saturation region of both the polarization and strain. There is also marked grain size dependence of both the dielectric constant and the field-induced strains for a given electric field. Larger grains have greatly improved dielectric constant and field induced strain levels. Near the dielectric constant maximum temperature the field induced strain for the BTS (.90/.10) composition was shown to be nearly temperature independent

Summary and Future Work

Developments of a data base continued for the optimization of the relaxor ferroelectric families with regard to sonar transducer applications i.e., their dielectric, polarization, and electromechanical properties. By delineating the regions of (I). Electrostrictive (II). Micro-Macro

and (III). Piezoelectric (remnant polarization) behavior for the electrostrictive compositional families, trends were established for compositional modifications.

Strain measurements were performed as a function of frequency up to moderate levels (1 KHz) and under prestressed load conditions for ceramic compositions. Load lines (strain/force) indicate that sizable strains can be achieved in relaxors while pushing significant (MPa) loads.

Property measurements for this report had a primary focus on determining by dielectric and polarization characterization for the various groups, the regimes of operation which can be used to predict the electromechanical response in those temperature region. Ongoing investigations will primarily focus upon the continuation of electromechanical property evaluations in the frequency range (10^2-10^3 Hz) at field levels of 10KV/cm and above, strain/force behavior under stress loading, and the completion of the dielectric polarization, P-E, S-E, data base for the groups which have been . Initial indications based upon laser strain interferometer measurements suggest that there is some dispersion of the field-induced strain for PLZT compositions.

The possible advantages for certain applications of the $Ba(Ti,Sn)O_3$ materials have been pointed out: low field linearity of the strain response, high effective electrostrictive coefficients, and the possibility of compositions with relatively small temperature dependence of maximum strain, These possible advantages have to offset the smaller levels of strain. Group III (BTS) ceramics prepared under differing sintering conditions and thus varied grain size will be examined for the effect which this will have upon the dielectric constant and field induced strains. Computation of the effective field dependence electrostrictive coefficients and higher frequency measurements are also being undertaken for this family.

References

PMN-PT and PLZT

1. T.R. Shrout and Joseph Fielding, Jr., "Relaxor Ferroelectric Materials," Proc. IEEE (1990).

2. Z.Y. Meng, U. Kumar, and L.E. Cross, "Electrostriction in Lead Lanthanum Zirconate-Titanate Ceramics," J. Amer. Ceram. Soc. 68, [8], p. 459-62 (1985).

3. K. Uchino, S. Nomura, L.E. Cross, and R. E. Newnham, "Electrostriction in Perovskite Crystals and its Application to Transducers," J. Phys. Soc. Jpn. [49], p. 45-48, Supp. B (1980).

4. N. Kim, "The Role of Lanthanum Modification on the Fabrication and Properties of Lead Magnesium Niobate-Lead Titanate Ceramics," M.S. Thesis, The Pennsylvania State University (1990).

5. W.Y. Pan, W.Y. Gu, D.J. Taylor, and L.E. Cross, "Large Piezoelectric Effect Induced by Direct Current Bias in PMN:PT Relaxor Ferroelectric Ceramics, Jpn. JAP 28, [4] p. 653 (1989).

6. Q.M. Zhang, S.J. Jang, and L.E. Cross, "High-frequency strain response in ferroelectrics and its measurement using a modified Mach-Zender interferometer," J. Appl. Phys. 65 [7], p. 2807 (1989).

$Ba(Ti,Sn)O_3$ (BTS)

7. G.A. Smolenskii and V. A. Isupov, Zh. tekh. Fiz. 24, p. 1375 (1954).

8. J. Von Cieminski, "Modeling of High-Signal Electrostriction. I-II," Z. Naturforsch, 45a, p. 1090 (1990).

9. J. Von Cieminski, H. Th. Langhammer, H.-P. Abicht, "Peculiar Electromechanical Properties of Some $Ba(Ti,Sn)O_3$ Ceramics," phys. stat. sol. (a) 120, p. 185 (1990).

10. J. Von Cieminski and H. Beige, "High Signal Electrostriction in Ferroelectric Materials," J. Phys. D: Appl. Phys. 24, p. 1182 (1991).

List of Figures

TABLE III(a)

Group I. PMN-PT: Cation A-Site Modification

Composition	Sintering Temperature (°C)	Depolar. Temp.T_d (°C)	T_{max} (°C) (1KHz)	$\|T_{max}-T_d\|$ (°C)	K_{max} (x 10^3)	tan δ_{max} (1 KHz)
PMN	1250°/2 Hrs.	-78.1	-9.95°	68.15	17.99	.10/ @ -24°
.98PMN-02PT	1250°/2 Hrs.	-58	5.2°	62.2	19.07	.095/@ 11°
.97PMN-.03PT	1250°/2 Hrs.	-45	9.45	54.45	21.55	.09/@ 2°
.95PMN-.05PT	1250°/2 Hrs.	-27	17.59	44.6	24.28	.10/@12°C
.93PMN-.07PT	1250°/2 Hrs.	-9	27.5	36.5	24.97	.095@19.8
PLMN	1200°/2 Hrs.	---	-35°	---	14.4	.11/@-47°
.95PLMN-.05 PT	1250°/2 Hrs.	-80	-7.06	72.96	19.0	.09/@ -15°
.93 PLMNM - .07 PT	1250°/2 Hrs.	-69	4.75	74.75	22.68	.11/@ -9°
.65 PMN-.35 PT: 7% La	1250°/2 Hrs.	-55°	13.5	68.6	13.70	.05/@ 7°

TABLE III(b)
B-Site Modification

Composition	Sintering Temperature	Depol. Temp. (°C)	T_{max} (°C)	$\lvert T_{max}-T_d \rvert$	($x10^3$) K_{max}	tan δ_{max} (@1KHz)
.93PMN - .07PT: Sr 1%	1200°/2 Hrs.	-50.5	9.3	59.8	20.21	.105 @-5
.93PMN - .07PT: Sr 3%	1200°/2 Hrs.	-115	-16.57	98.43	18.4	.12 @ -38
.93PMN - .07PT: Sr5%	1200°/2 Hrs.	-135	-22.81	112.19	16.5	.116 @ - 44.2
.85PMN- .15PT/Ba 1%	1200°/2 Hrs.	23	59.5	36.5	22.9	
.85 PMN- .15PT/Ba 3%	1200°/2 Hrs.	29	39.0	10	18.4	
.85 PMN- .15PT/Ba 5%	1200°/2 Hrs.	---	19	---	17.45	

Table III(c)

PNN-PZT Compositions	T_d	Region II $\lvert T_{max}-T_d \rvert$	T_m	Kmax	tanδ max	Temp @ tanδ max
.80 PNN-20 PZT	-165	225.71	-40.71°	11.27	.0836	-55.46
.75 PNN-.25 PZT	-127	111.38	-15.62°	11.96	.0888	-44.13
.70 PNN - .30 PZT	-82	100.15	8.15°	14.21	.0798	-17.22

Table 4 Group II. PLZT (X/65/35)

Dielectric / Polarization (@ 1 KHz)	PLZT (9/65/35) 1200°C/1200*°C	(10/65/35) 1200/1200C*	11/65/35 1200°/1200C*°
K_{max} (°C) (x 10^3)	7.6/7.80	6.9/7/12	5.3/5.31
T_{max} (°C)	84.4/77°	53.2/54.9	39°/39.0
T_d (°C)	/-31°	/-69.1°	/-102°
T_{max}-T_d	/108°	/124°	/141°
tan δ_{max} / Temp. (1 KHz)	/.062 @ 36°	/.074 @ 19°	/.075 @ 1.2°

* Annealed at 900°C for 6Hrs. in air.

Table 5. $Ba(Ti_{0.87}Sn_{0.13})O_3$ Transverse Strain Properties

Temp	Strain (με) (10 KV/cm)	Strain (με) (20KV/cm)	% Hysteresis
31°C	32	77	<0.5 %
19°C	59	110	1.5%
12°C	91	140 με	2.5%
7°C	127	185	3%
12°C	123	179/	6%
-9°C	108	170 με	7.5%
-13°C	111	104/158	11%

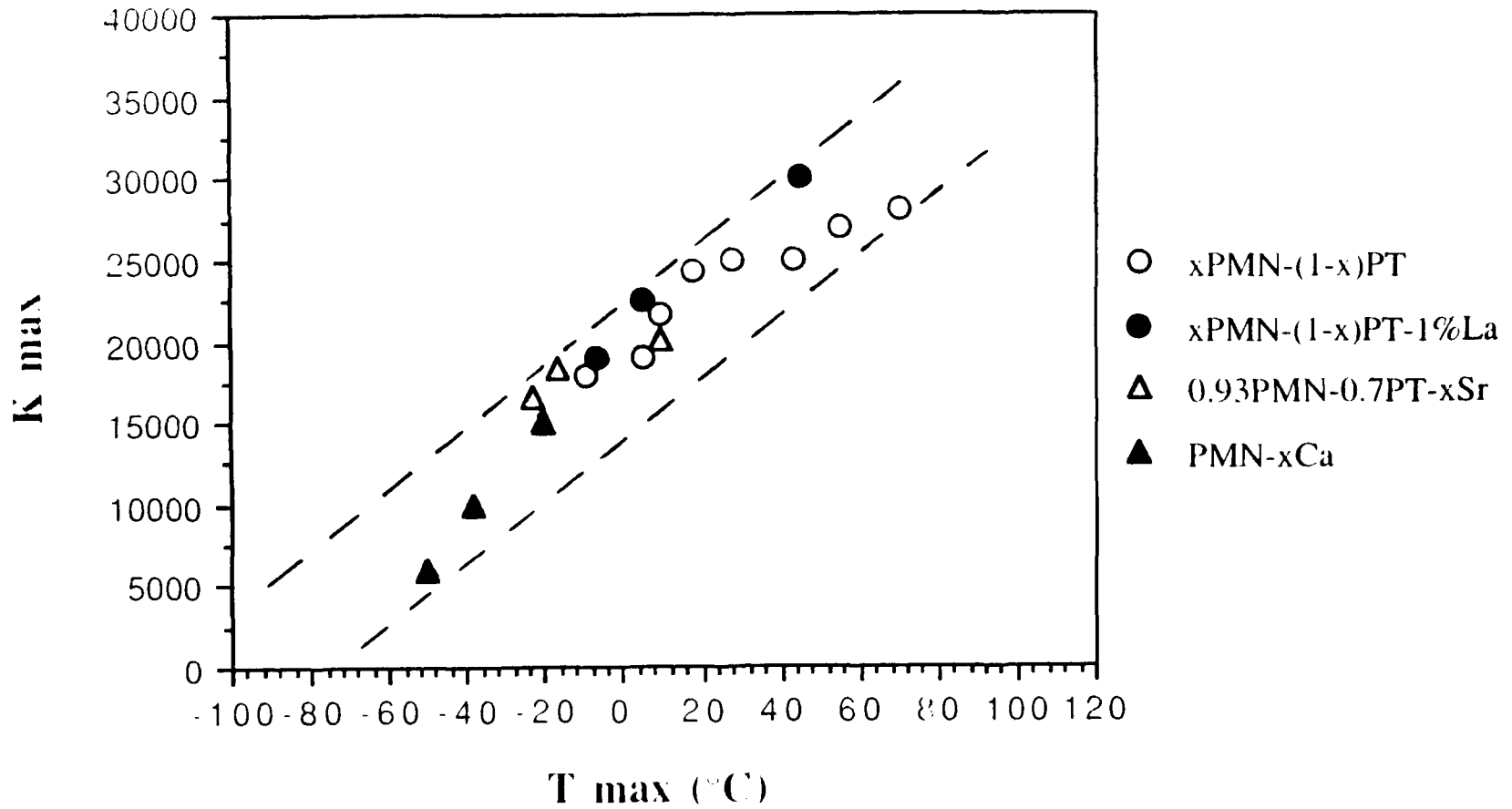

Figure 1 Dielectric constant maximum (K_{max}) as a function of dielectric constant maximum temperature (T_m) for the PMN based Group I relaxors with cation modifications

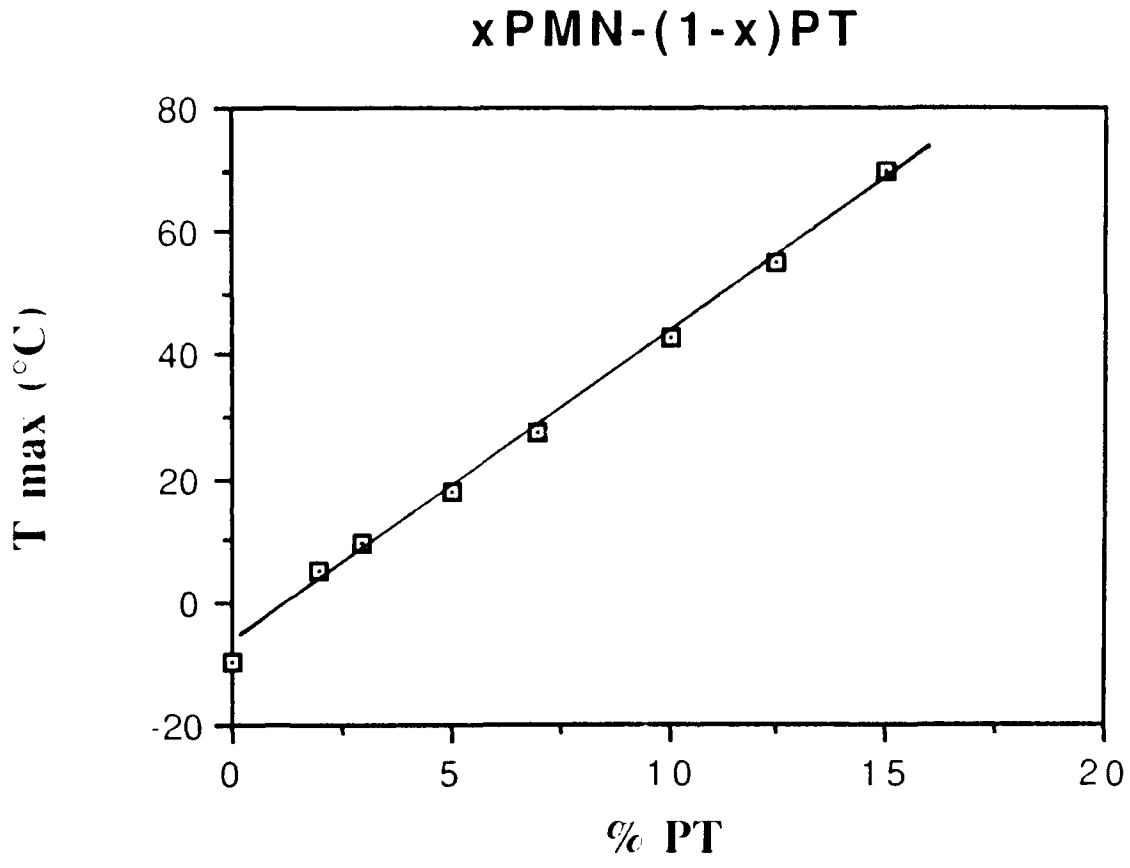

Figure 2 Dielectric constant maximum (K_{max}) as a function of $PbTiO_3$ content for the PMN-PT compositions.

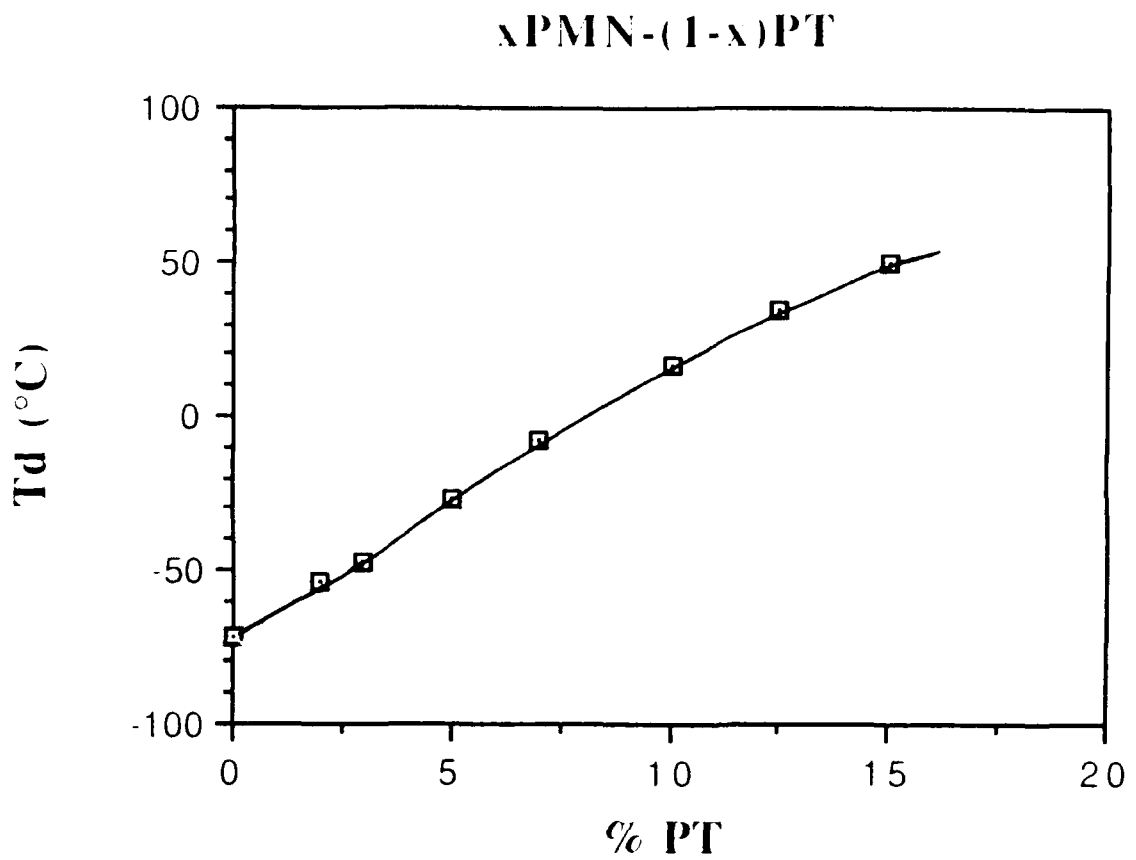

Figure 3 Depolarization temperature (T_d) of the polarization as a function of $PbTiO_3$ content for the PMN-PT compositions.

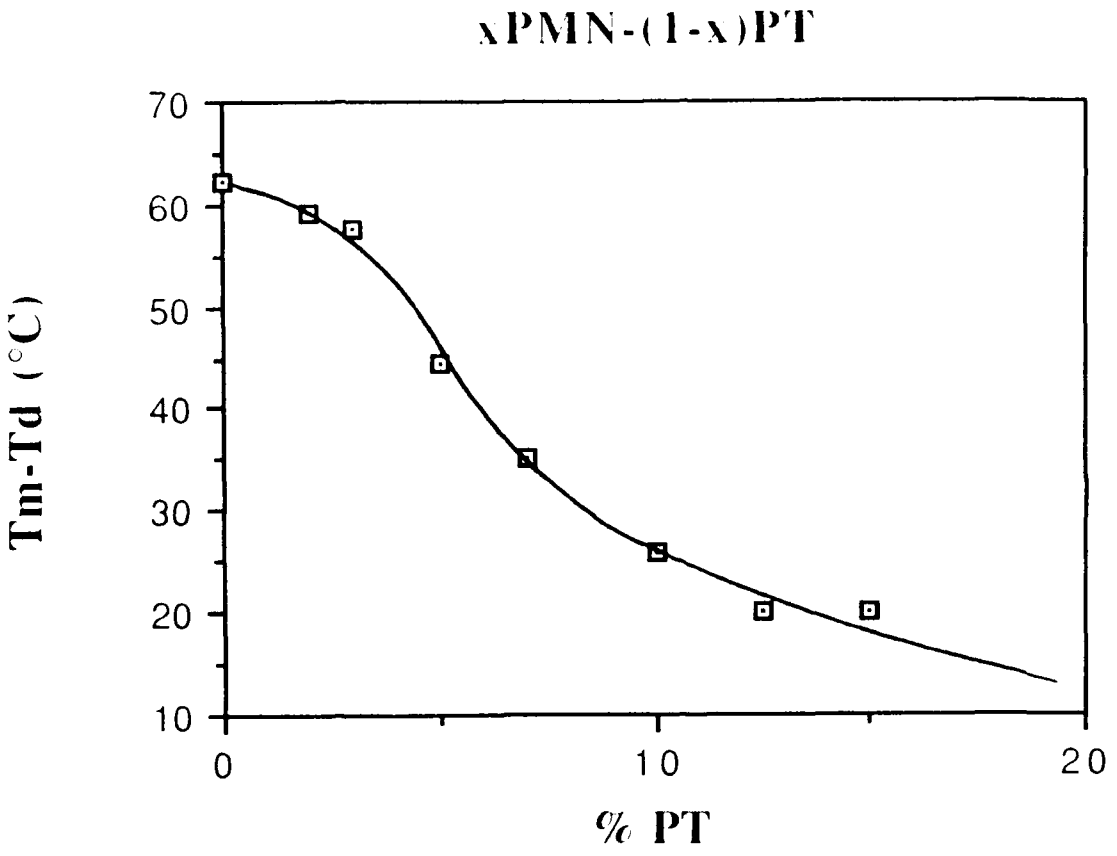

Figure 4 The difference between the depolarization temperature (T_d) of the polarization and dielectric constant maximum temperature (T_m) as a function of $PbTiO_3$ content for the PMN-PT compositions.

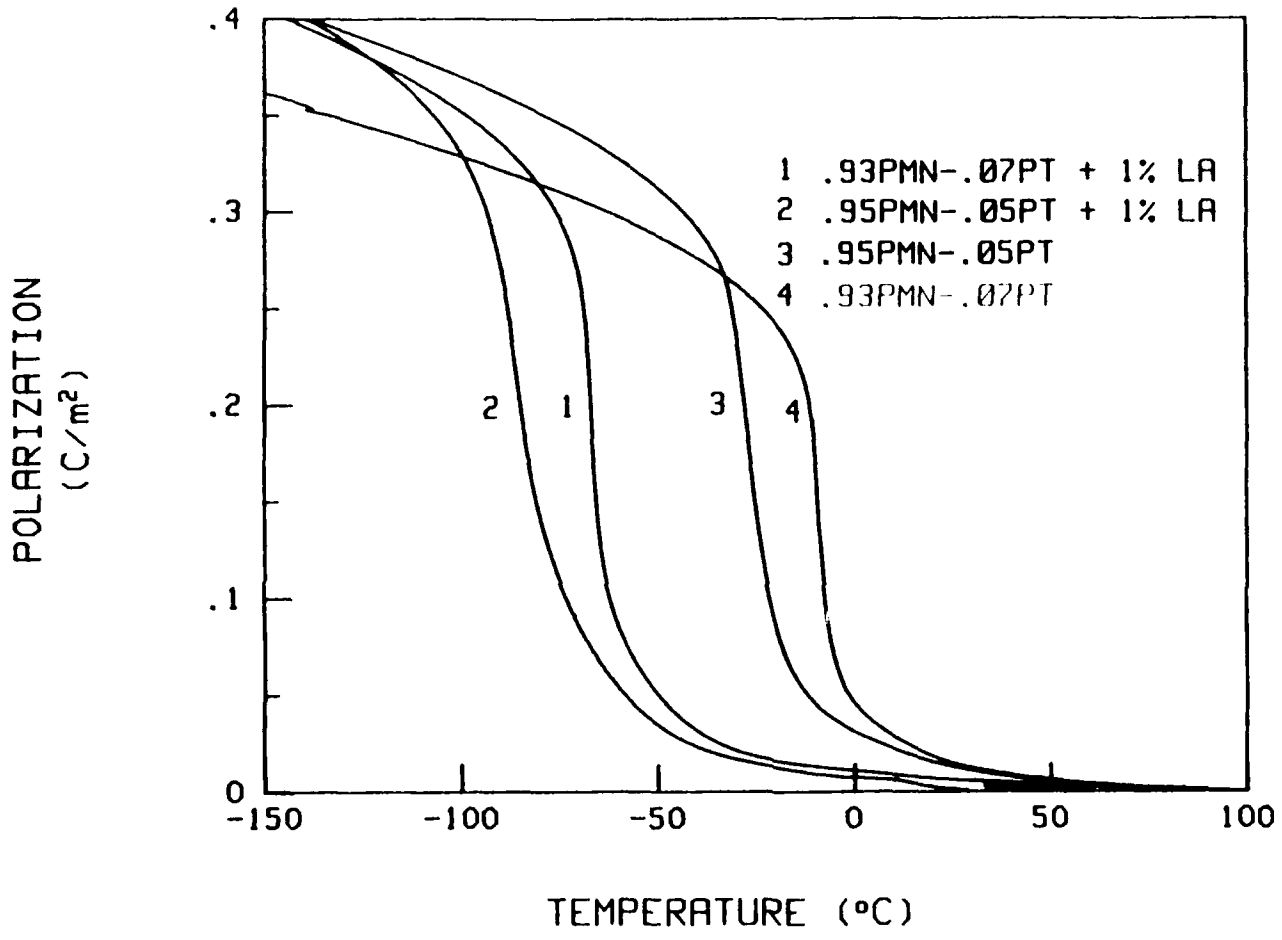

Figure 5 Polarization (P) as a function of temperature for some PMN-PT and PLMN-PT compositions.

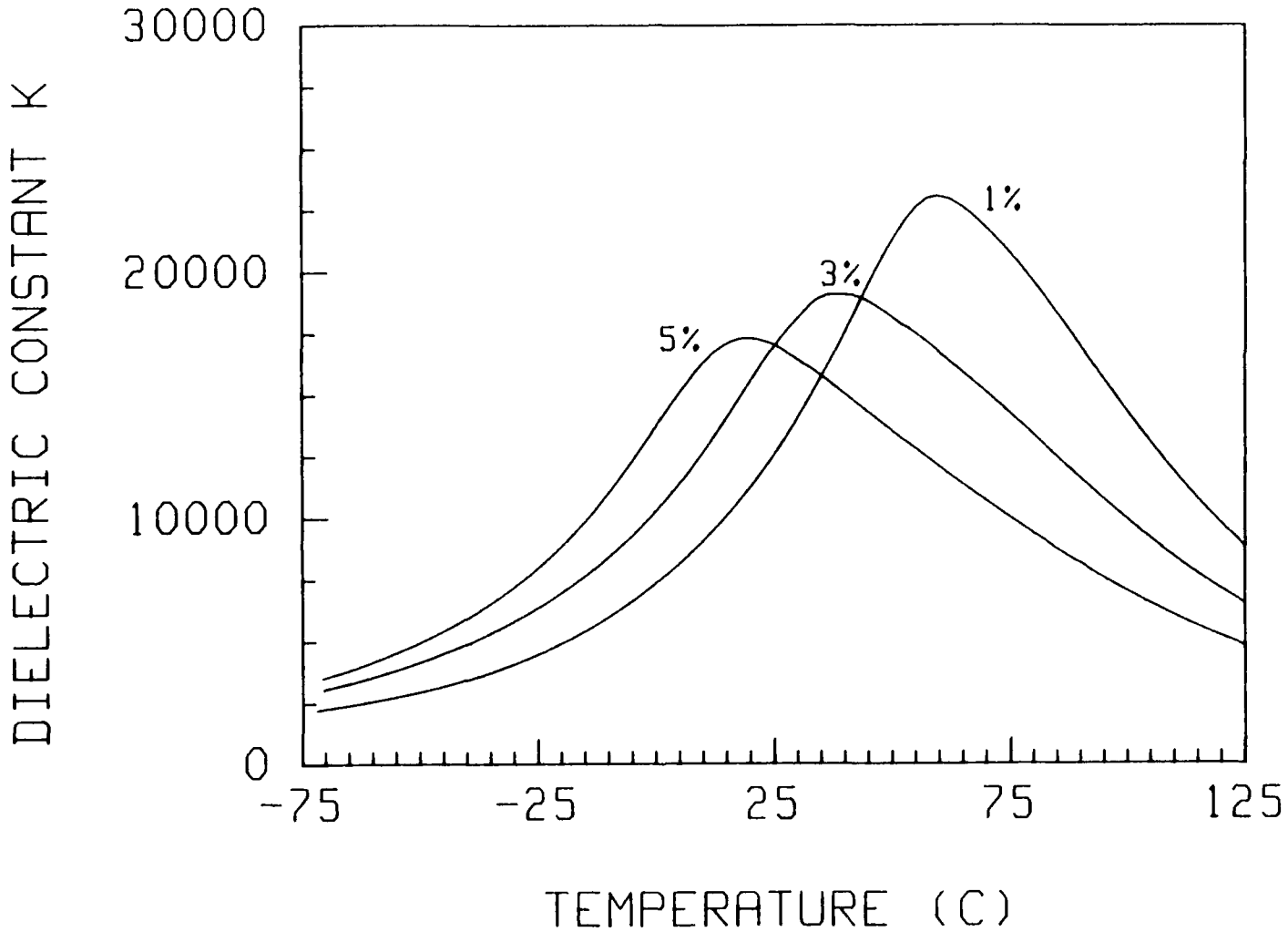

A) PMN-PT-BA

Figure 6 The dielectric constant (K) as a function of temperature illustrating the effect of Ba (1,3,5% addition) on a) .85PMN-.15PT b) .75PMN-.25PT.

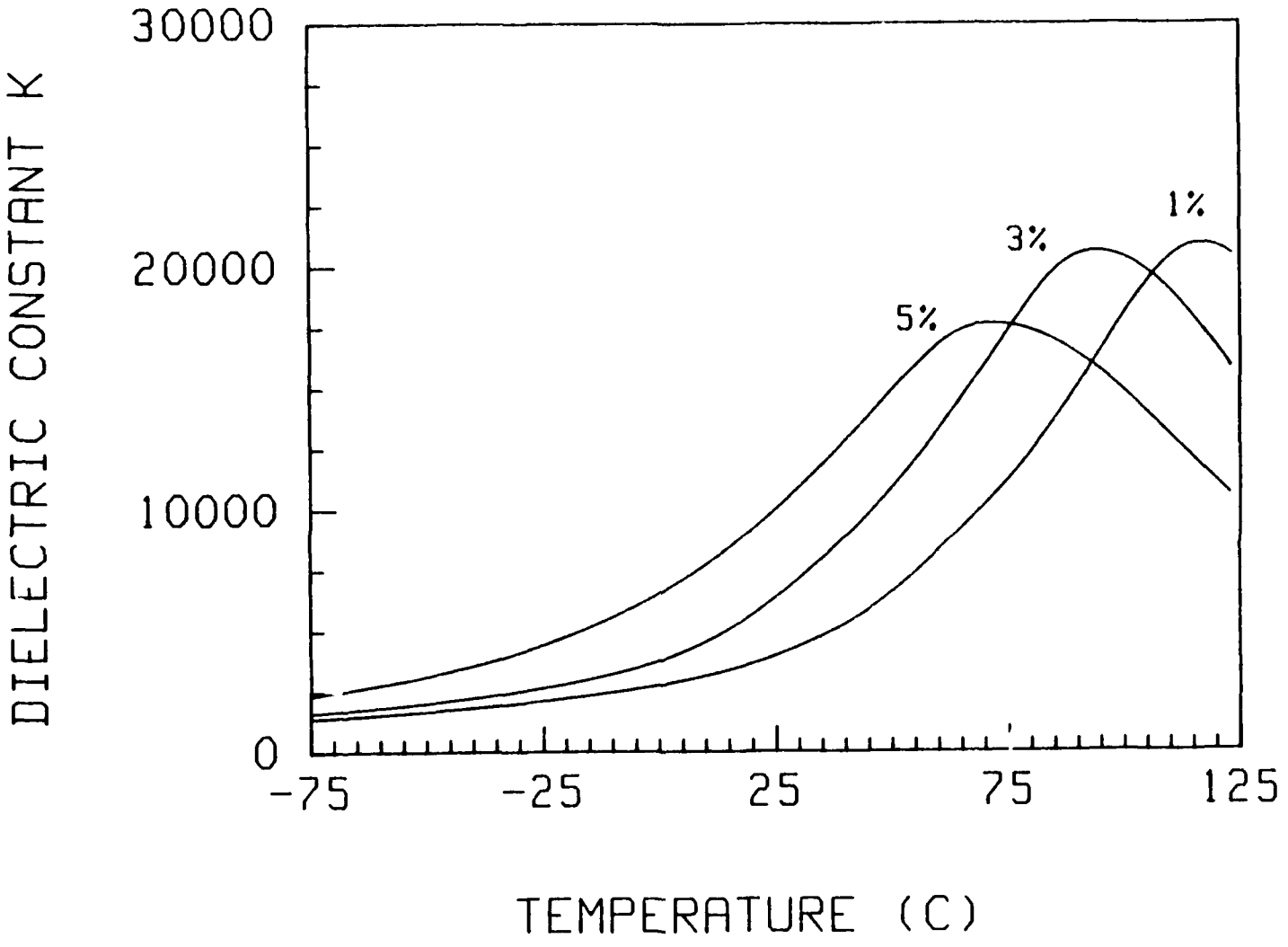

B) PMN-PT 75/25 WITH 1,3 AND 5 MOL% BA SUBSTITUTIONS

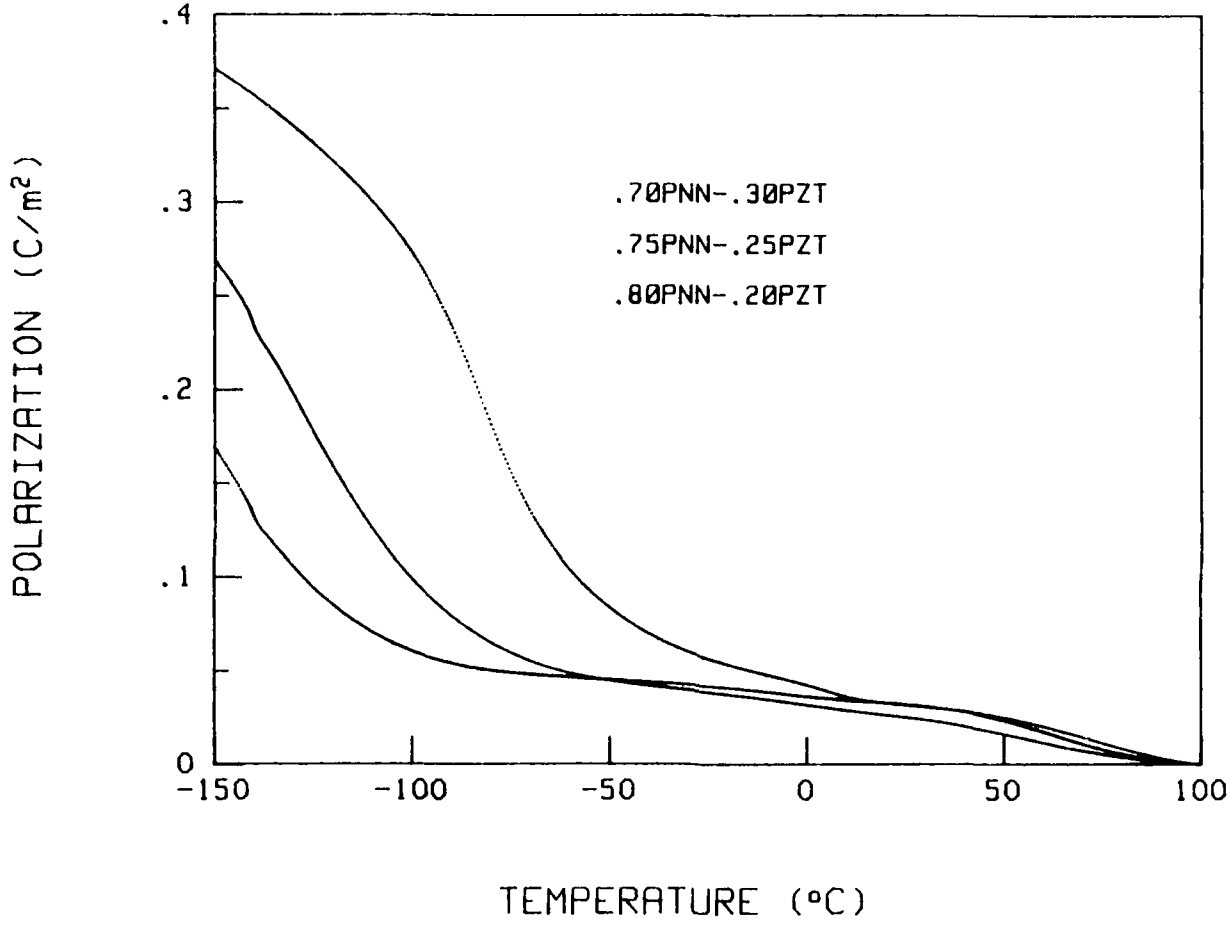

Figure 7 Polarization (P) as a function of temperature for PNN PZT compositions.

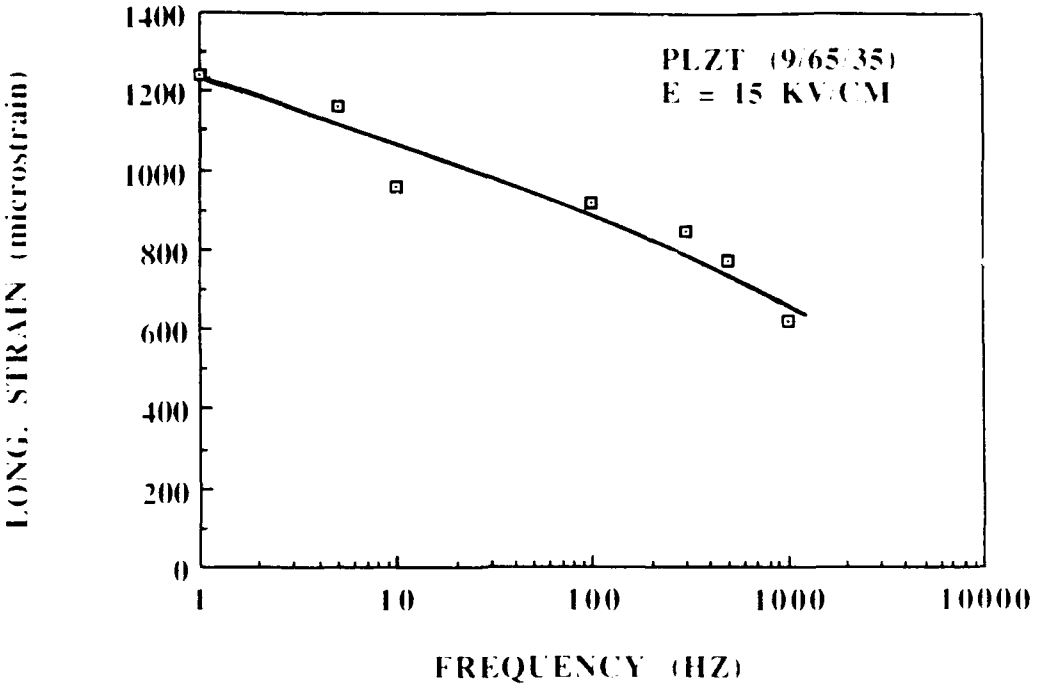

Figure 8 Longitudinal Strain for PLZT (9/65/35) at 15 kV/cm electric field as a function of frequency as measured by the strain ultradilatometer.

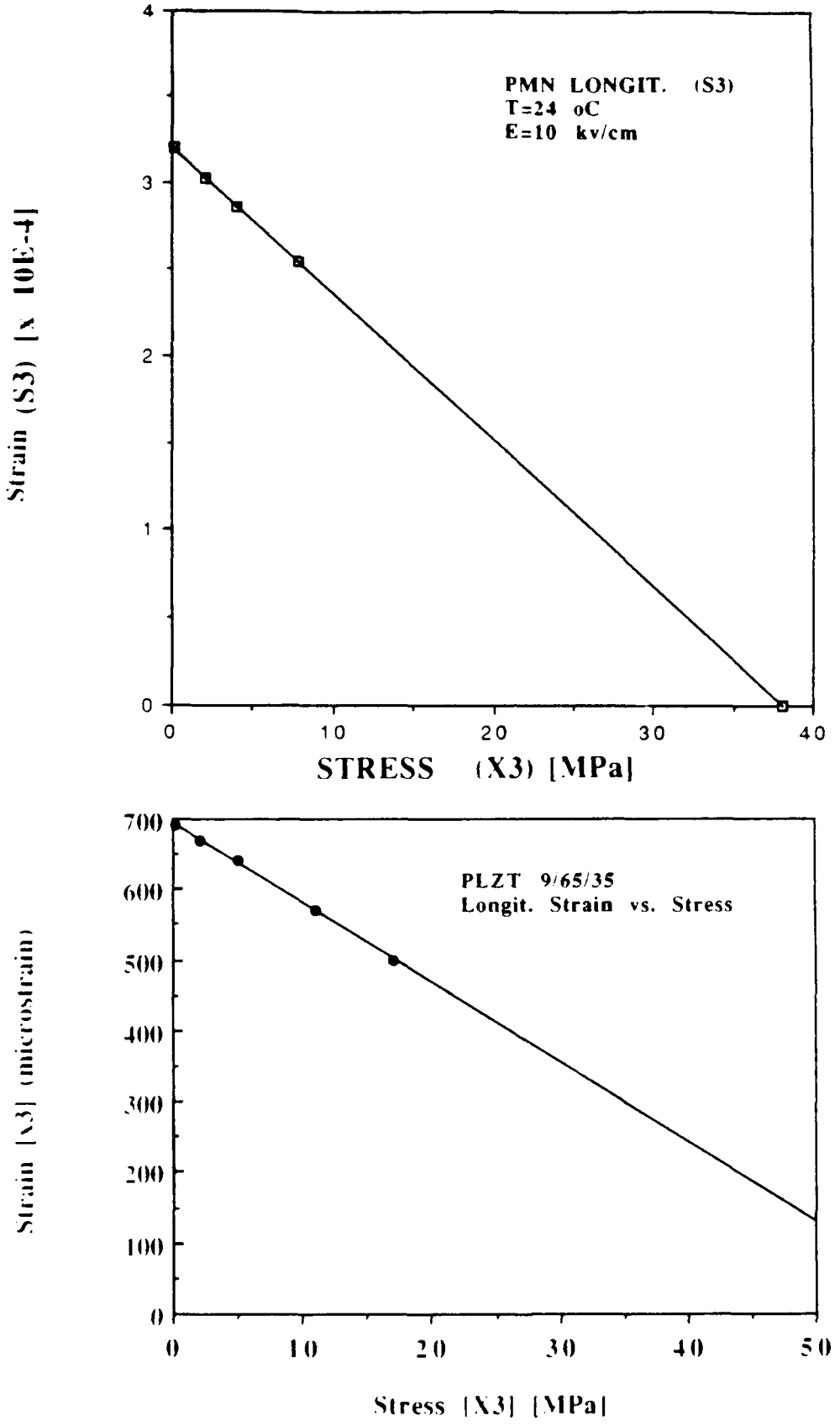

Figure 9 Longitudinal Strain vs. Stress Loadlines for PMN and PLZT (9/65/35) at 10 kV/cm electric field calculated using measured elastic compliances and measured strains.

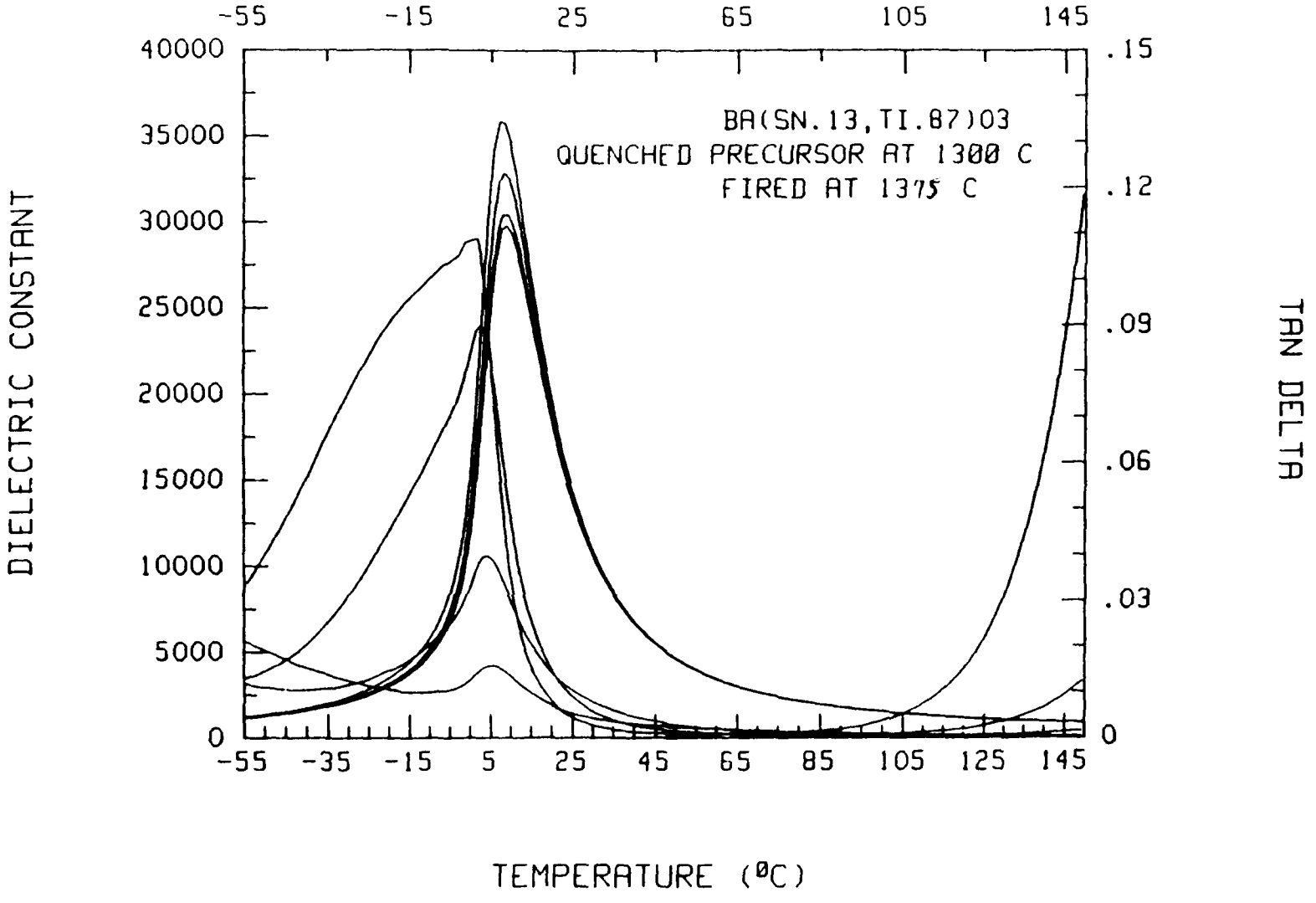

Figure 10 The dielectric constant (K) as a function of temperature for $Ba(Ti_{.87}Sn_{.13})O_3$

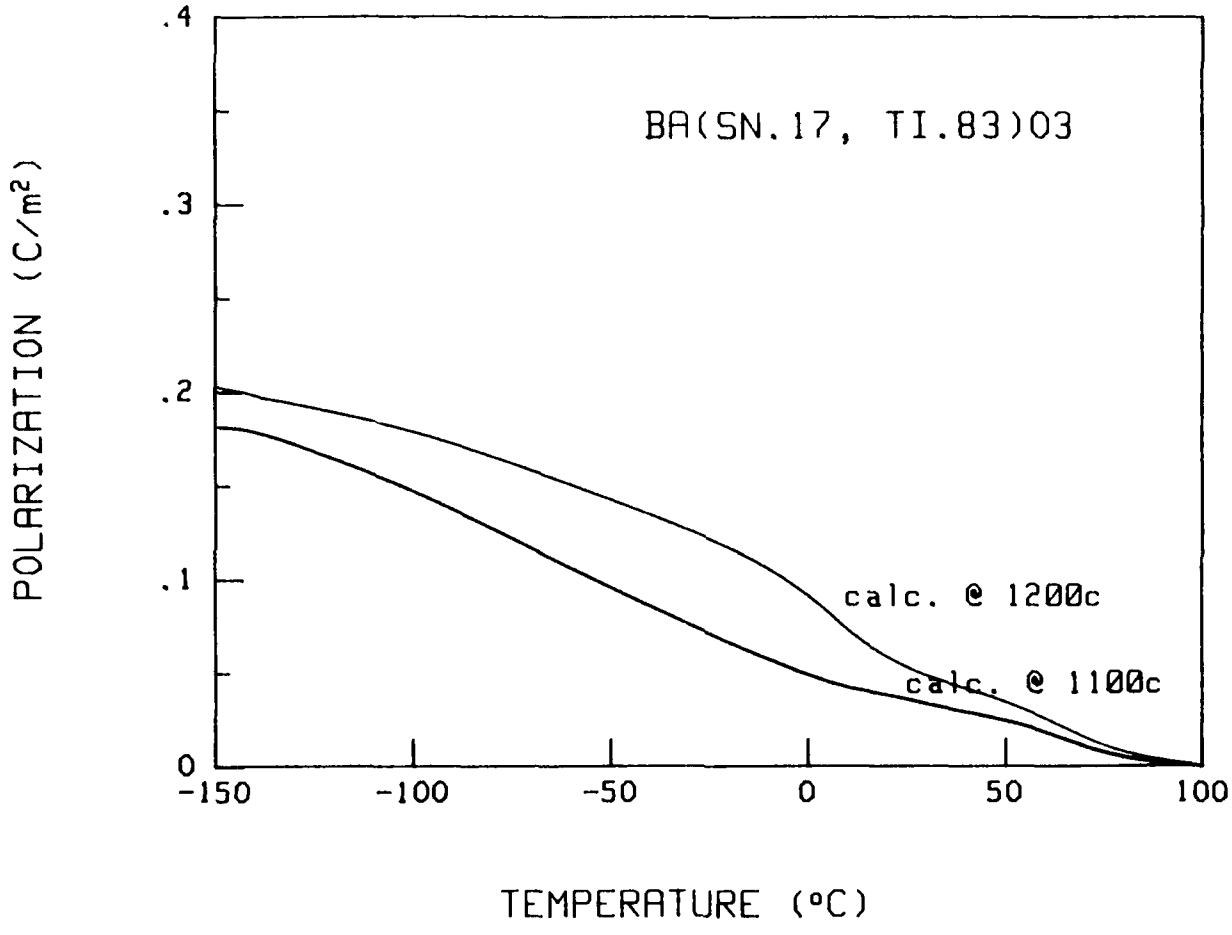

Figure 11 Polarization (P) as a function of temperature for $Ba(Ti_{.87}Sn_{.13})O_3$

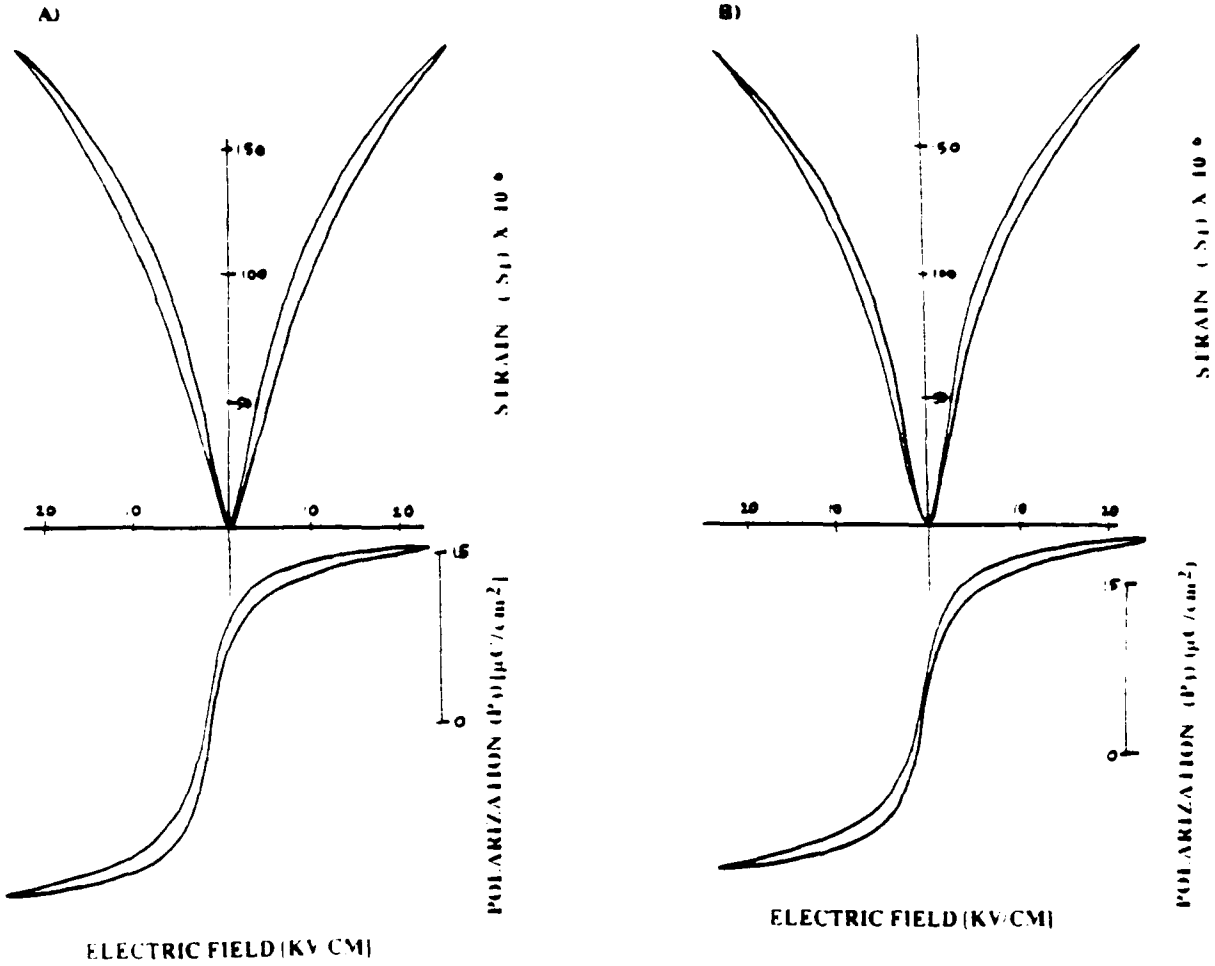

Figure 12 Transverse strain and dielectric polarization hysteresis loops as a function of electric field for $Ba(Ti_{.87}Sn_{.13})O_3$ at the temperatures a) -13 °C b) 2 °C c) 12°C d) 19 °C e) 31°C.

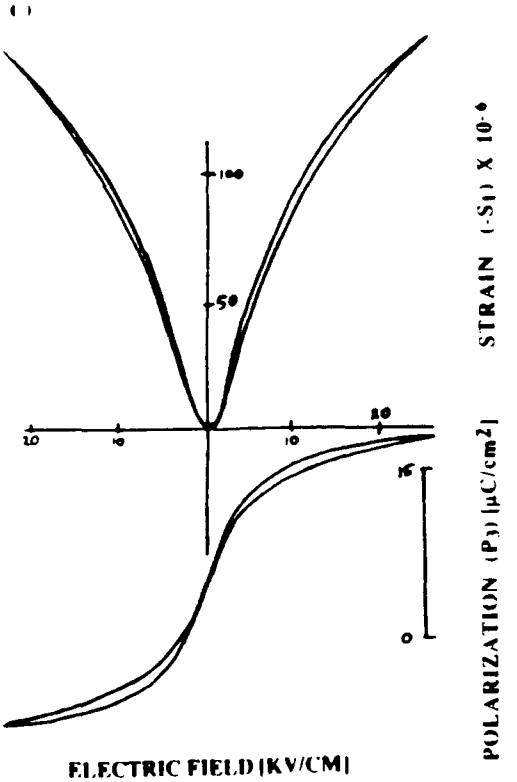
100
50
20
10
5
10
20
15
0
STRAIN (-S1) X 10⁻⁶
POLARIZATION (P3) (μC/cm²)
ELECTRIC FIELD (KV/CM)

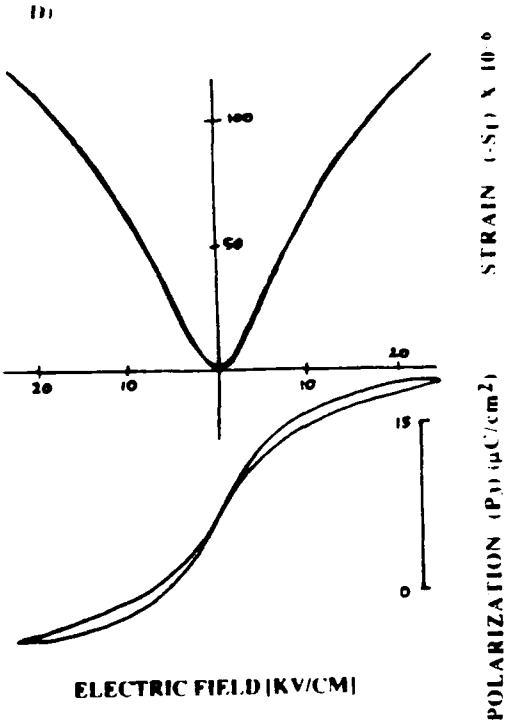
100
50
20
10
10
20
15
0
STRAIN (-S1) X 10⁻⁶
POLARIZATION (P3) (μC/cm²)
ELECTRIC FIELD (KV/CM)

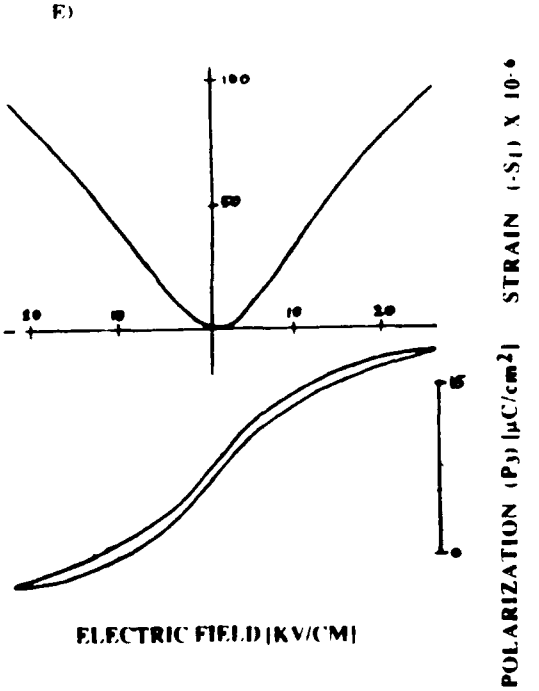
100
50
20
10
20
15
0
STRAIN (-S1) X 10⁻⁶
POLARIZATION (P3) (μC/cm²)
ELECTRIC FIELD (KV/CM)